Heat Transfer in Shrouded Rectangular Cavities

M. K. Chyu,* D. E. Metzger,† and C. L. Hwan‡
Arizona State University, Tempe, Arizona

Heat transfer with turbulent flow over shrouded rectangular cavities is numerically investigated. The geometry studied models flow through the clearance gap at the grooved tip of an axial turbine blade, where the blade rotates in close proximity to a stationary outer ring or shroud. The direction of the relative shroud motion is always in opposition to the direction of the gas flow across the blade tip. The heat transfer characteristics and flow pattern in a cavity are found to be strongly influenced by the dimension of the gap clearance, cavity geometry, and relative shroud movement.

Nomenclature

C = height of clearance gap
C_u = constant in turbulence model, = 0.09, Eq. (3)
D = cavity or groove depth
h = convective heat transfer coefficient, $= q/(T_w - T_i)$
k = turbulence kinetic energy
k_f = fluid heat conductivity
Nu = local Nusselt number, $= hC/k_f$
$\overline{Nu}$ = area-averaged Nu over cavity floor
$\overline{\overline{Nu}}$ = area-averaged Nu over entire cavity and surfaces upstream and downstream of cavity
q = wall heat flux
Re = Reynolds number, $= \rho UC/\mu$
S_ϕ = source term for a dependent variable, Eq. (1)
T = temperature
T_i = temperature at inlet of clearance gap
T_w = wall temperature
u = velocity component in x direction
U = streamwise velocity at inlet of clearance gap
U_s = shroud velocity in x direction
W = cavity width in streamwise direction
x = cavity floor coordinate
x_r = reattachment length
y = cavity sidewall coordinate
Γ_ϕ = effective transport coefficient for dependent variable
ϵ = dissipation rate of turbulence kinetic energy
μ = fluid dynamic viscosity
ρ = fluid density
σ_ϕ = effective Prandtl number, Eq. (2)
ϕ = dependent variable in computation

Introduction

IN gas turbines, the blades of axial turbine stages rotate in close proximity to a stationary peripheral wall (sometimes termed an outer ring or stationary shroud). The differential expansion of the turbine wheel, blades, and shroud causes variations in the size of the clearance gap between the blade tip and stationary shroud. The necessity to tolerate this differential thermal expansion dictates that the clearance gap cannot be eliminated altogether, despite accurate engine machining.[1]

Pressure differences between the pressure and suction sides of a blade drive a flow through the clearance gap. This flow, often referred to as the "tip leakage" flow, is detrimental to the engine performance. The primary detrimental effect of the tip leakage flow is the reduction of turbine stage efficiency, and a second important effect concerns the convective heat transfer associated with the flow. The surface area at the blade tip in contact with the hot working gas represents an additional thermal loading on the blade which, together with heat transfer to the suction- and pressure-side surface areas, must be removed by the blade's internal cooling flows.[2]

Very limited information on turbine tip heat transfer and fluid flow has been reported to date,[3-6] and almost all of the published work dealing with clearance gap flows involves the consideration of only plain flat blade tips. However, a strategy commonly employed to reduce tip flow and heat transfer is the grooving of a single rectangular cavity chordwise along the blade tip. The groove acts like the cell of a labyrinth seal to increase the pressure drop and thus reduce the flow for a given pressure differential across the tip. The reduction of the flow will of course act to reduce heat transfer. A schematic diagram representing the geometry of a grooved blade tip, viewed from a coordinate system fixed relative to the blade is shown in Fig. 1. The outer shroud can be considered moving in the general direction from the suction side to the pressure side, with relative velocity equal to U_s. The leakage flow, denoted by U, is driven by the pressure difference between two sides of the blade and flows in the direction opposite to the shroud motion. With this general configuration in mind, the grooved tip problem can be categorized as the fluid flow and heat transfer over a shrouded rectangular cavity.

Both the fluid flow and the heat transfer over unshrouded, rectangular cavities have been the subjects of extensive investigation for many years.[7] The flowfield over a cavity is characterized by flow separation and shear layer reattachment resulting in complex flow patterns with substantial effects on the friction drag and heat transfer. Most studies have relied on flow visualization techniques and/or heat and mass transfer data to obtain momentum and heat transfer information in a cavity flow.[8-10] Several researchers have studied cavity flows using finite-difference methods to solve the governing elliptic equations.[11] However, almost all of the numerical studies are limited to two-dimensional configurations in the laminar flow regime. In all cases, the cavity problems previously studied have been considered as a flow system in which the cavity is open to a usually well-specified approaching flow over an otherwise smooth and stationary surface. The approaching

Received May 19, 1986; revision received Oct. 15, 1986.

*Assistant Professor, Department of Mechanical and Aerospace Engineering. Member AIAA.
†Professor and Chairman, Department of Mechanical and Aerospace Engineering. Member AIAA.
‡Graduate Assistant, Department of Mechanical and Aerospace Engineering.

flow may be a wall boundary layer for external flow or a well-developed channel flow.

The grooved tip differs from the aforementioned unshrouded situation by virtue of the confined nature of the geometry as well as by the proximity of the moving shroud. The degree of similarity between the heat transfer characteristics of the grooved tip and those of previous cavity studies has been unclear until recently. Metzger and Bunker,[12] using a time-dependent paint-coating technique, studied the heat transfer for a flow through a confined narrow slot-type channel where one of the bounding walls contains a rectangular cavity. The effect of shroud motion is not included in their study. Details of heat transfer on the cavity surfaces are found to be largely dependent on the size of the gap opening and the cavity aspect ratio. A semiempirical study by Mayle and Metzger,[6] using a plain-tip geometry, has argued that the heat transfer from the blade tip is essentially unaffected by the relative motion between the blade and the shroud. This speculation, however, has not been justified for the grooved-tip situation. To gain further understanding of the convective heat transfer in cavities with various degrees of relative shroud motion is the primary objective of this paper.

Heat transfer for the turbulent airflow over a two-dimensional, shrouded cavity is numerically investigated herein. A computer program based on a finite-difference method and the standard, high-Reynolds number $k-\epsilon$ turbulence model is developed for the computation. The testing cases are: the gap to cavity width ratio, $C/W=0.05$, 0.1, 0.15; the cavity depth to width ratio, $D/W=0.1$, 0.2, 0.5; the relative shroud moving speed, $U_s/U=0$, -1, -4; and the Reynolds number based on the inlet mean velocity and the gap height, $Re=\rho UC/\mu=10^4$ and 1.5×10^4. Information gained from this study should improve the understanding of the nature of the flow and heat transfer in the grooved-tip region. It should also support more rational and optimal design choices for improvements in future turbine engines.

Numerical Computation

A control-volume-based finite-difference method is employed for solving a system of partial differential equations describing the conservation of mass, momentum, energy, and turbulent flowfields. The formulation entails an elliptic system of equations for properly describing the separated, recirculating flow. The computer program uses the SIMPLER (SIMPLE-Revised) algorithm[13] to solve explicitly for the velocity and pressure fields. The turbulent parameters are determined by a two-equation, k-ϵ model in association with a ramp-type wall function.[14] The momentum, continuity, and turbulence equations, together with their coupling characteristics, constitute five equations to be solved simultaneously for the converged velocity field. This is followed by the separate solution of the energy equation. For a computational domain similar to that shown in Fig. 1, the computation uses a 40×26 grid for all cases studied and a nonuniform spacing with dense placement near solid walls. A typical run on an IBM 3081 mainframe computer takes approximately 250 iterative steps for a converged velocity field, and an additional 30 steps are required for the temperature computation.

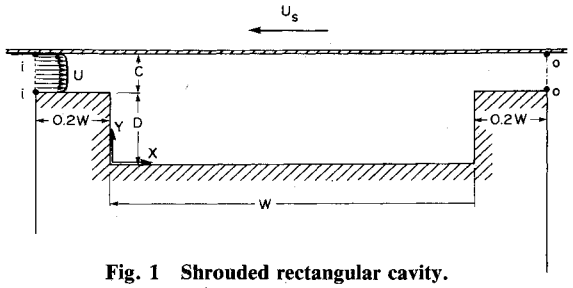

Fig. 1 Shrouded rectangular cavity.

In the two-dimensional rectangular $(x-y)$ coordinate system, the governing equation for a statistically stationary, steady-state turbulent flow can be written in the following general form:

$$\frac{\partial}{\partial x}(\rho u\phi)+\frac{\partial}{\partial y}(\rho v\phi)=\frac{\partial}{\partial x}\left(\Gamma_\phi\frac{\partial\phi}{\partial x}\right)+\frac{\partial}{\partial y}\left(\Gamma_\phi\frac{\partial\phi}{\partial y}\right)+S_\phi \quad (1)$$

where ϕ denotes any dependent variable in its time-averaged value. S_ϕ is a source term that includes all the terms that are not covered by the first four terms (representing the convective and diffusive contributions). Γ_ϕ is the effective transport coef-

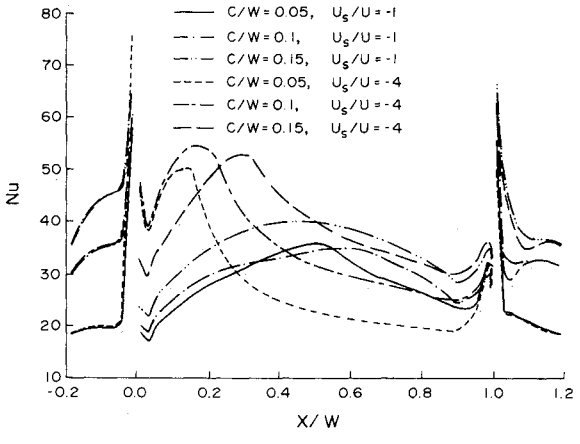

a) $D/W=0.1$.

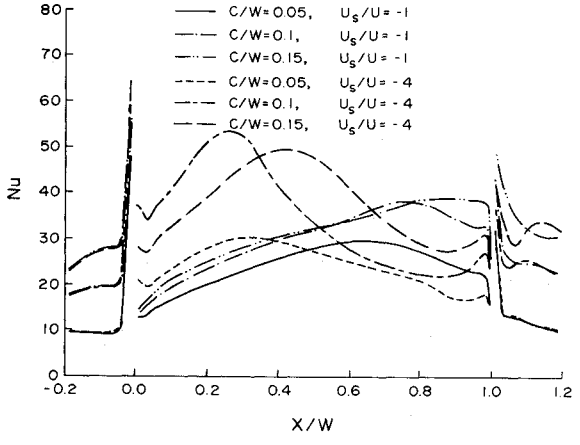

b) $D/W=0.2$.

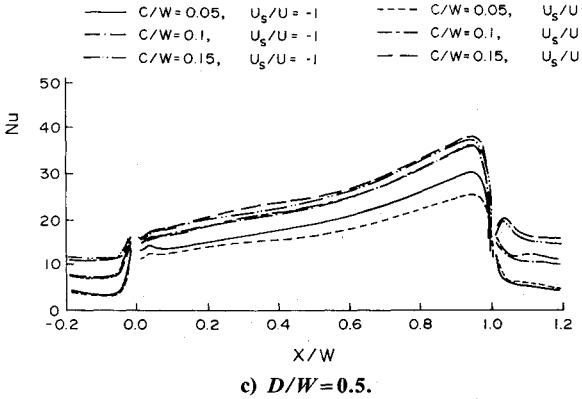

c) $D/W=0.5$.

Fig. 2 Local Nu distribution in streamwise direction; $C/W=0.1$, $Re=1.5\times10^4$.

ficient for the variable ϕ and is given by

$$\Gamma_\phi = \mu_{\text{eff}}/\sigma_\phi \tag{2}$$

where μ_{eff} is the effective viscosity in the flowfield and σ_ϕ is the corresponding effective Prandtl number for each ϕ. The effective viscosity is determined based on the hypothesis that the turbulent transport is the predominant feature and the molecular diffusion is practically negligible, so that $\mu_{\text{eff}} = \mu_t$. The turbulent viscosity μ_t can be obtained from the values of the time-averaged, turbulence kinetic energy (k) and its dissipation (ϵ), using

$$\mu_t = C_u \rho k^2/\epsilon \tag{3}$$

where C_u is taken to be a constant equal to 0.09. The dependent variables of interest are u, v, k, ϵ, and T. The details of the transport coefficient and corresponding source term for each dependent variable are listed in Table 1.

There are several different versions of the k-ϵ model,[14-16] and some of them are ad hoc in nature, with different empirical constants or additional source terms. The particular version chosen in this study is the so-called "high Reynolds number k-ϵ model", which is considered to be the most efficient with regard to computing time and storage. Previous studies in the literature have shown that the model is very effective in providing results that are in good agreement with experimental data for a variety of flow situations. Prior to the actual computations for shrouded cavities, the computer program was used to caculate the flowfield and heat transfer for a turbulent, fully-developed channel flow. The results were in excellent agreement with those in the literature, and this provided confidence in the present study.

For the flowfield computation, no-slip boundary conditions are imposed along the solid walls, a zero normal gradient is imposed at the outlet of the computational domain (plane o-o' in Fig. 1), and a uniform velocity profile with $u = U$ and $v = 0$ is specified at the inlet (plane $i-i'$ in Fig. 1). It is arguable that this inlet condition may be inappropriate to model the actual turbine situations. Flow separation likely exists near the gap inlet due to the sharp angle of entrance. However, because detailed information on the flow pattern and turbulence parameters at the inlet is lacking, exact flow modeling near this region appears to be difficult if not impossible. In addition, variations of blade geometry and operating conditions in gas turbines should produce differences in the inlet flow pattern, so that a too specific modeling may be even more improper for this study. Thus, the most general and fundamental case is chosen—uniform profile.

The temperatures at the gap inlet and solid walls are specified as T_i and T_w respectively. A Prandtl number equal to 0.7 is used to represent air as the flow medium. The standard logarithmic wall function treatment[14] is used near the walls for the parallel velocity components, the temperature, and the turbulence parameters k and ϵ.

Results and Discussion

A sample of results describing the local Nu distribution on the cavity floor and surfaces upstream and downstream to the cavity is shown in Fig. 2. The figure consists of three parts, representing $Re = 1.5 \times 10^4$ and covering $D/W = 0.1$, 0.2, 0.5, $C/W = 0.05$, 0.1, 0.15, and $U/U_s = -1$, -4. It is found that for the present range of parameters, the curves for U_s/U between 0 and -1 are virtually indistinguishable, having at most a 3% variation in corresponding local values of Nu. Hence, the results for $U_s/U = -1$ can also be regarded as the representatives for the case with a stationary shroud. In other words, the speculation in Ref. 6 that relative shroud motion has an indiscernible effect on the blade-tip heat transfer is supported by the present computational results, at least for $U_s/U \leq -1$.

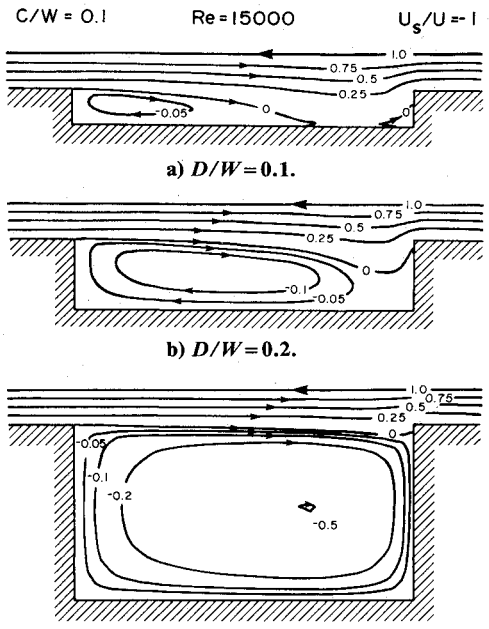

Fig. 3 Contours of stream function; $U_s/U = -1$, $C/W = 0.1$, $Re = 1.5 \times 10^4$.

Table 1 Governing equations

Equation	ϕ	Γ_ϕ	S_ϕ
Continuity	1	0	0
x momentum	u	μ_t	$-\frac{\partial p}{\partial x} + \frac{\partial}{\partial x}\left(\mu_t \frac{\partial u}{\partial x}\right) + \frac{\partial}{\partial y}\left(\mu_t \frac{\partial v}{\partial x}\right)$
y momentum	v	μ_t	$-\frac{\partial p}{\partial y} + \frac{\partial}{\partial x}\left(\mu_t \frac{\partial u}{\partial y}\right) + \frac{\partial}{\partial y}\left(\mu_t \frac{\partial v}{\partial y}\right)$
Turbulence kinetic energy	k	μ_t/σ_k	$G - \rho\epsilon$
Turbine energy dissipation	ϵ	μ_t/σ_ϵ	$(C_1 G - C_2 \rho\epsilon)(\epsilon/k)$
Temperature	T	μ_t/σ_t	0

$$G \equiv \mu_t \left\{ 2\left[\left(\frac{\partial u}{\partial x}\right)^2 + \left(\frac{\partial v}{\partial y}\right)^2 \right] + \left(\frac{\partial u}{\partial y} + \frac{\partial v}{\partial x}\right)^2 \right\}$$

$$\sigma_k = 1,\ \sigma_\epsilon = 1.3,\ \sigma_t = 0.9,\ C_1 = 1.44,\ C_2 = 1.92$$

On the surface upsteam of the cavity, the heat transfer characteristics depend on the geometry of the cavity located downstream of the surface and the gap spacing. However, the influence of shroud motion on the heat transfer in this portion of the surface is also found to be negligible. In general, the value of Nu increases with a decrease of D/W and an increase of C/W. This geometrical dependency for the surface upstream to a cavity is expected to be attenuated when the value of C/W is sufficiently large. In the limiting case without a shroud, i.e., $C/W \to \infty$, it is indeed found to be the case in a recent experimental study by Chyu and Goldstein.[10] As seen in Fig. 2, except for the deepest cavity, i.e., $D/W = 0.5$, the Nu on the surface upstream of the cavity increases with the streamwise location and reaches a sharp maximum near the downstream edge of the surface. This increasing trend of Nu may be attributed to the level of turbulence in the near-wall

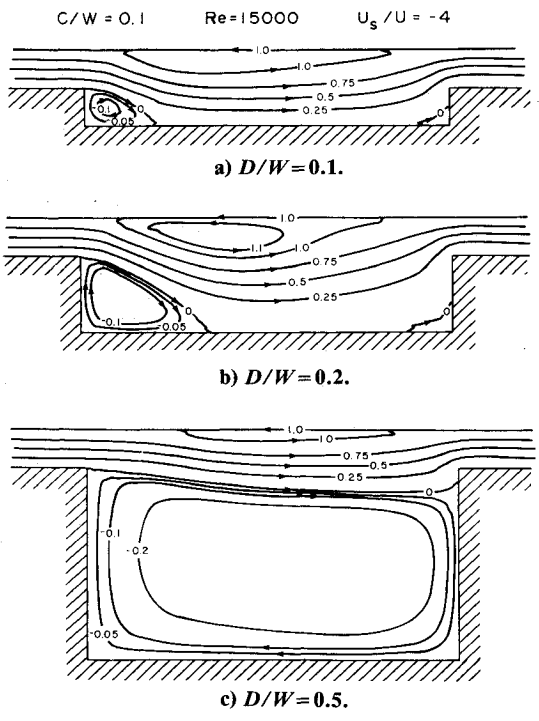

Fig. 4 Contours of stream function; $U_s/U=-4$, $C/W=0.1$, $Re=1.5\times10^4$.

region, which increases along the streamwise direction. The location at which the maximum *Nu* occurs is near the top corner of the cavity downstream-facing wall (upstream wall), where flow separates and a highly turbulent shear layer starts to develop downstream.

Heat transfer characteristics from the surface downstream of the cavity are similar to those of a newly developing boundary layer with zero angle of incidence. In contrast to the surface upstream to the cavity, the highest *Nu* occurs near the leading edge of the surface. For a given Reynolds number, the variation of *Nu* is similar to that for the surface upstream to the cavity with the same values of C/W and D/W; i.e., *Nu* increases as C/W increases and D/W decreases. The influence of the shroud speed on the heat transfer behavior is found to be more significant for this surface than for the surface upstream to the cavity. For $U_s/U=0$ and -1, *Nu* decreases monotonically with the downstream position; however, for higher relative shroud movement, i.e., $U_s/U=-4$, a local maximum *Nu* is to be found in the midportion of the surface. The latter appears to be more significant with a cavity of large C/W and small D/W. Under these conditions, the highly turbulent shear layer originating from the cavity upstream wall is permitted to grow wider and to generate more turbulence in the layer before it impinges the cavity downstream (upstream-facing) wall. At least part of this highly turbulent layer is deflected toward the cavity top, gaining a velocity component normal to the mainstream direction after the impingement, due mainly to the pressure difference between the region of impingement and the mainstream. The flowfield in this region is therefore similar to that of a sharp-edged boundary-layer development, and a second maximum heat transfer downstream of the leading edge is often observed.

The most drastic influences of shroud motion on the heat transfer over the entire computational domain are on the cavity floor. The heat transfer from the cavity surfaces is closely related to the flow pattern in the cavity. A recirculating region, which is enveloped by the dividing streamline separated from the top edge of the cavity upstream wall and the solid wall boundary, exists immediately downstream of the cavity upstream wall. For an unshrouded cavity, previous studies have reported that the dividing streamline reattaches at the cavity floor, provided that the cavity is sufficiently wide, say $D/W\leq0.1$;[9] otherwise, it will reattach at the cavity downstream side-wall. The streamwise distance between the cavity upstream wall and the location of reattachment is commonly termed the "reattachment length," x_r. In the near region upstream to the floor reattachment, the turbulent kinetic energy as well as the turbulent viscosity reaches a maximum value, as does the local heat transfer coefficient. Another recirculation, but with a weaker strength, is frequently observed in the lower corner immediately ahead of the cavity downstream wall, provided that the floor reattachment exists.

The present results, as shown in Figs. 3 and 4, typify the foregoing description of the flow pattern within a cavity. The flow pattern is found to be strongly dependent on the values of D/W and U_s/U, and it is little influenced by variations in either C/W or Reynolds number. Also shown in Figs. 3 and 4 are contours of the computed stream function representing the characteristic flow patterns for the cases of $C/W=0.1$, $Re=1.5\times10^4$, $D/W=0.1$, 0.2, and 0.5, and $U_s/U=-1$ and -4, respectively. For $U_s/U=-1$, the floor reattachment only occurs for $D/W=0.1$, and the recirculation fills the entire cavity for the other two D/W values. The corresponding heat transfer behavior is revealed in Fig. 2. For $D/W=0.1$ and $U_s/U=-1$, *Nu* increases along the streamwise direction, reaches a local maximum near the reattachment point, and then decreases downstream. The local maximum *Nu* occurs approximately 0.1 to $0.2W$ upstream of the flow reattachment point ($x_r\simeq0.8W$), and this spatial difference appears to be proportional to the magnitude of C/W. For $D/W=0.5$, as a contrast to the case of $D/W=0.1$, *Nu* increases monotonically along the streamwise direction until it reaches the cavity downstream wall; no midfloor maximum exists. For $D/W=0.2$, the general characteristic of *Nu* vs x/W depends on the value of C/W. For $C/W\geq0.1$, the cavity floor *Nu* for $D/W=0.2$ shows a similar characteristic to that of $D/W=0.5$; otherwise, as seen in Fig. 2b, its local maximum occurs at 0.7 W from the cavity upstream wall.

The flow pattern changes when the relative shroud motion increases. The dominant effect due to the additional shear furnished by the opposed moving shroud is another recirculating region atop the cavity and immediately adjacent to the moving shroud. The other effect is a reduction in the streamwise dimension of the recirculating region, which strongly influences the heat transfer behavior in the cavity. This recirculation-size reduction is evidenced by a comparison between Figs. 3a and 4a for $D/W=0.1$; x_r decreases from 0.75 to $0.25W$ as the magnitude of U_s/U increases from -1 to -4. Furthermore, from Figs. 3b and 4b for $D/W=0.2$, it is noted that with $U_s/U=-4$, the dividing streamline reattaches at the cavity floor at $x_r=0.4W$, whereas no floor reattachment exists for $U_s/U=-1$.

The variations in the flow pattern affect the heat transfer characteristics on the cavity floor accordingly. As shown in Fig. 2a, for $D/W=0.1$, the location of the local maximum *Nu* occurs at a location more upstream for $U_s/U=-4$ ($0.15W$) than for $U_s/U=-1$ (0.55W). In addition, the value of the maximum *Nu* for $U_s/U=-4$ is approximately 30–40% higher as compared to $U_s/U=-1$. This increase can be explained by examining the influence of U_s/U on the velocity field and turbulent diffusivities inside the cavity. According to the computed results, the local velocity is higher for an increased relative shroud movement and is also accompanied by the higher turbulent diffusivity in the recirculating region and near the reattachment point. Downstream of the reattachment point, the cavity floor *Nu* for $U_s/U=-4$ drops sharply and eventually becomes lower than that for $U_s/U=-1$. Downstream of the reattachment, the wall shear stress generally decreases in the downstream direction and a new boundary layer begins to grow up through the reattached shear layer. An increase in shroud movement resulting in an

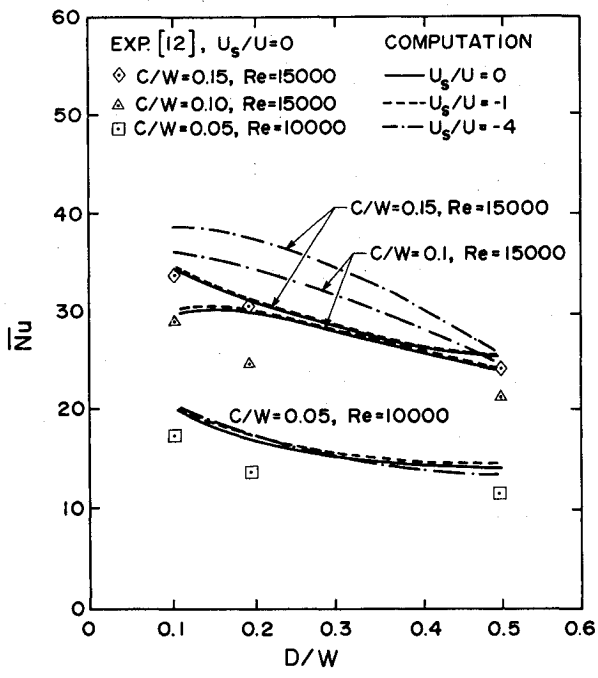

Fig. 5 Area-averaged *Nu* over cavity floor.

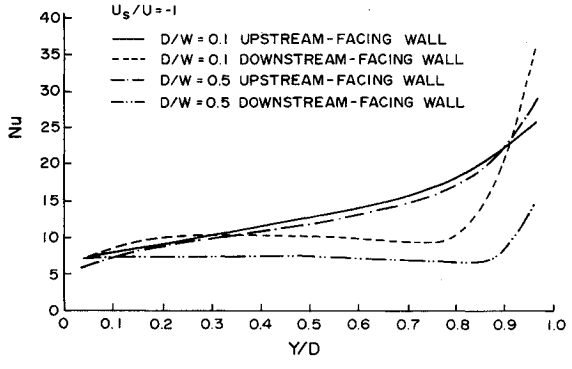

Fig. 6 Local *Nu* on cavity side walls, $U_s/U=-1$, $C/W=0.1$, $Re=1.5\times10^4$.

increase in opposed shear in the mainstream, decreases the favorable pressure gradient along the streamwise direction in the aft-reattachment portion of the cavity floor. This effect retards the local velocity, thickens the boundary layer, and suppresses the convective heat transfer.

The degree of the influence of the shroud movement on the heat transfer from the cavity floor depends on both the gap size and the cavity aspect ratio, i.e., C/W and D/W. It is understandable that, with the same flow condition and D/W, the smaller value of C/W experiences the stronger effect of shroud movement on the cavity heat transfer. As seen in Fig. 2a for $D/W=0.1$, $C/W=0.05$ has the lowest values of *Nu* distributed on the cavity floor downstream of the reattachment. Similar characteristics are also found for $D/W=0.2$ and 0.5, as shown in Figs. 2b and 2c. However, there is no sharp increase of *Nu* on the floor upstream portion for $D/W=0.5$, simply because no reattachment occurs on the floor. For a deep cavity, in general, a thin, separated shear layer bridges the entire cavity and the external flow skims past the cavity without a strong interaction with the flow inside. Thus, despite the difference in shroud motion, the floor *Nu* for $D/W=0.5$ virtually has the identical distribution on the cavity floor for $C/W=0.1$ and 0.15, as shown in Fig. 2c. For $C/W=0.05$, the shroud motion effect becomes more significant and causes the lower values of *Nu* for $U_s/U=-4$ than for $U_s/U=-1$.

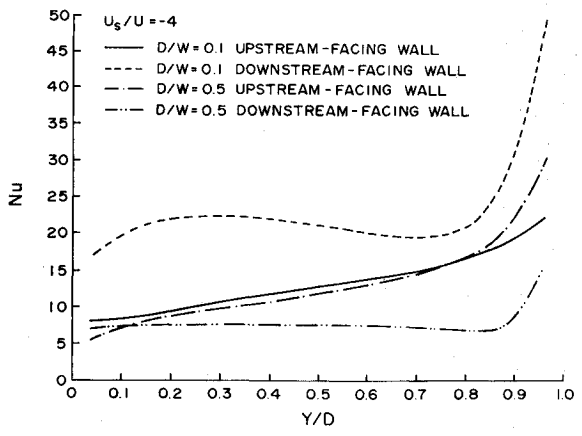

Fig. 7 Local *Nu* on cavity side walls, $U_s/U=-4$, $C/W=0.1$, $Re=1.5\times10^4$.

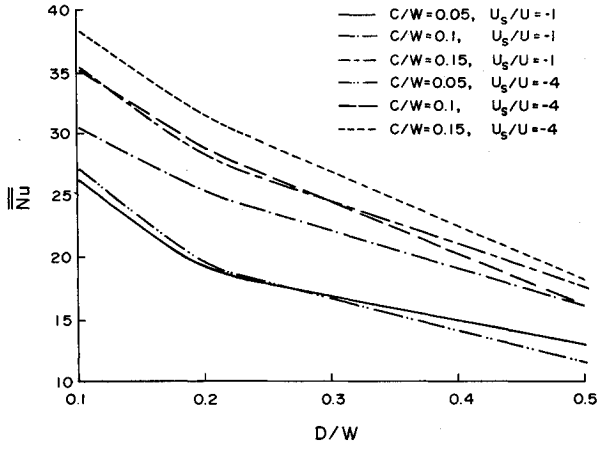

Fig. 8 Area-averaged *Nu* over entire cavity and surfaces upstream and downstream of cavity.

Figure 5 shows the area-averaged Nusselt number over the cavity floor, $\overline{Nu}$. The general trend is that $\overline{Nu}$ increases with increases in *Re*, C/W, and the magnitude of U_s/U, and a decrease in D/W. Among all the cases studied, the combination of the lower Reynolds number, the highest shroud moving speed, and the deepest cavity results in the lowest average floor Nusselt number. The experimental results with a stationary shroud obtained in Ref. 12 are also presented as open symbols in the figure. Computed and measured values of $\overline{Nu}$ are agreeable, although the computational results are generally higher. Excellent agreement is found for situations with the widest gap clearance ($C/W=0.15$), and about 10–15% deviation exists for the narrowest gap cases ($C/W=0.05$). The largest difference between the measured and computed results is less than 20%, i.e., for $C/W=0.1$ and $D/W=0.2$. To be noted is that the geometries and flow conditions in the experiment[12] and the present computation are not exactly the same. First, the inlet condition is different, which has been discussed previously. Second, in the experiment, the test rig is essentially a three-dimensional cavity, and discrepancies are expected when using a two-dimensional model.

Figures 6 and 7 show the Nusselt number along the cavity sidewalls for $U_s/U=-1$ and -4, respectively. For an unshrouded cavity, the fundamental mode of heat transfer for the upstream-facing wall is the impingement of the shear layer on the wall and generally results in a higher heat transfer coefficient as compared to a downsteam-facing wall. The results shown in Fig. 6 for a smaller relative shroud motion, $U_s/U=-1$, apparently support this notion. The opposite trend is found when the shroud movement increases, par-

ticularly for a shallow cavity. As shown in Fig. 7, the values of Nu on the downstream-facing wall surpass those on the upstream-facing wall, except near the top region for $D/W=0.5$. The heat transfer on the downstream-facing wall is dominated by the recirculating region attached behind the wall. The increasing shroud motion enhances the turbulent mixing effect in the recirculating region, as previously discussed, and is responsible for the results shown in Fig. 7.

Area-averaged Nusselt number, $\overline{Nu}$, over the entire cavity, including the surfaces upstream and downstream of the cavity, are presented in Fig. 8 for $Re=1.5\times10^4$. Without taking into account the difference in the heat transfer area associated with different cavity geometries, these results can be viewed as representing heat transfer on grooved-blade tips. For both a constant leakage flow rate and a constant relative shroud speed, higher overall heat transfer coefficients are found for the shallow cavity and wider clearance gap. Stronger relative shroud movement causes a higher overall heat transfer coefficient for a given value of C/W and $D/W\leq0.2$, and this effect appears to be more significant when C/W is large. However, the trend is attenuated with an increase of D/W, and it will eventually be reversed if the value of D/W is sufficiently large. As seen in Fig. 8, for $C/W=0.05$, $\overline{Nu}$ for $U_s/U=-1$ is higher than that for $U_s/U=-4$, provided that $D/W\geq0.25$. Similar results will occur for $C/W=0.1$ and 0.5 with larger values of D/W.

Conclusions

The effect of the magnitude of the relative shroud motion on the local heat transfer characteristics in shrouded cavities has been investigated numerically. The particular geometry chosen models the grooved tip of a rotating turbine blade moving in close proximity to a stationary outer ring or shroud. In this application, the direction of the relative shroud motion is always in opposition to the direction of the gas flow across the blade tip.

The present computed cases of $U_s/U=0$ and -1 are in all respects virtually identical. For $U_s/U=-1$, the effects of shroud motion are confined to a thin layer adjacent to the shroud, and the cavity region flow patterns, mean velocities, turbulent diffusivities, and heat transfer coefficient distributions are unaffected. For $U_s/U=-4$, however, the strong shroud motion, apparently aided by the flow area increase provided by the presence of the cavity, precipitates a region of flow separation immediately adjacent to the shroud and directly above the cavity. The separated flow region acts to deflect the throughflow toward the cavity floor, producing dramatic changes in overall flow patterns, reattachment points, and heat transfer coefficient distributions.

Acknowledgment

The present work was supported by a grant from NASA-Lewis within the framework of a research project on heat transfer near the tip region of a turbine blade.

References

[1]Hennecke, D. K., "Heat Transfer Problems in Aero-Engines," *Heat and Mass Transfer in Rotating Machinery,* edited by D. E. Metzger and N. H. Afgan, Hemisphere, Washington, DC, 1984, pp. 353–379.

[2]Metzger, D. E. and Mayle, R. E., "Gas Turbine Engines," *Mechanical Engineering*, Vol. 105, June 1983, pp. 44–52.

[3]Lakshminarayana, B., "Methods for Predicting the Tip Clearance Effects in Axial Flow Turbomachinery," *Transactions of ASME, Journal of Basic Engineering,* Vol. 92, 1970, pp. 467–482.

[4]Booth, T. C., Dodge, P. R., and Hepworth, H. K., "Rotor-Tip Leakage: Part I—Basic Methodology," *Transactions of ASME, Journal of Engineering for Power,* Vol. 104, 1982, pp. 154–161.

[5]Wadia, A. R. and Booth, T. C., "Rotor-Tip Leakage: Part II—Design Optimization Through Viscous Analysis and Experiment," *Transactions of ASME, Journal of Engineering for Power*, Vol. 104, 1982, pp. 162–169.

[6]Mayle, R. E., and Metzger, D. E., "Heat Transfer at the Tip of an Unshrouded Turbine Blade," *Proceedings of the 7th International Heat Transfer Conference*, Münich, West Germany, Vol. 3, 1982, pp. 87–92.

[7]Aung, W., "Separated Force Convection," Keynote Paper, ASME/JSME Thermal Engineering Conference, Honolulu, HI, March 1983.

[8]Haugen, R. L. and Dhanak, A. M., "Heat Transfer in Turbulent Boundary-Layer Separation over a Surface Cavity," *Journal of Heat Transfer*, Vol. 89, 1967, pp. 335–340.

[9]Yamamoto, H., Seki, N., and Fukusako, S., "Forced Convection Heat Transfer on Heated Bottom Surface of a Cavity," *Journal of Heat Transfer*, Vol. 101, 1979, pp. 475–479.

[10]Chyu, M. K., and Goldstein, R. J., "Local Mass Transfer in Rectangular Cavities with Separated Turbulent Flow," *Proceedings of the 8th International Heat Transfer Conference*, San Francisco, CA, Vol. 3, 1986, pp. 1065–1070.

[11]Bhatti, A. and Aung, W., "Finite Difference Analysis of Laminar Separated Forced Convection in Cavities," *Journal of Heat Transfer,* Vol. 106, 1984, pp. 49–54.

[12]Metzger, D. E., and Bunker, R. S., "Cavity Heat Transfer on a Grooved Wall in a Narrow Flow Channel," ASME Paper 85-HT-57, 1985.

[13]Patankar, S. V., *Numerical Heat Transfer and Fluid Flow*, Hemisphere, Washington DC, 1980.

[14]Launder, B.E. and Spalding, D. B., "The Numerical Computation of Turbulent Flows," *Computer Methods in Applied Mechanics and Engineering*, Vol. 3, 1974, pp. 269–289.

[15]Jones, W. P. and Launder, B. E., "The Prediction of Laminarization with a Two-Equation Model of Turbulence," *International Journal of Heat Mass Transfer*, Vol. 15, 1972, pp. 301–313.

[16]Leschziner, M. A. and Rodi, W., "Calculation of Annular and Twin Parallel Jets Using Various Discretization Schemes and Turbulence—Model Variations," *Journal of Fluids Engineering,* Vol. 103, 1981, pp. 352–360.